Acidity, Surface Structure, and Catalytic Performance of WO_x Supported on Monoclinic Zirconia

Thomas Onfroy, Guillaume Clet, and Marwan Houalla*

Laboratoire de Catalyse et Spectrochimie (UMR CNRS 6506), ENSICAEN-Université de Caen, 6 Bd. du Maréchal Juin, 14050 Caen (Cedex), France

Received: April 8, 2004; In Final Form: November 9, 2004

The relationship between the acidity, catalytic activity, and surface structure for tungsten oxide supported on zirconia was investigated for a series of solids prepared by equilibrium adsorption on monoclinic zirconia. The catalysts were active for propanol dehydration only above a threshold in W loading. The acidity was studied by infrared spectroscopy of adsorbed probe molecules (2,6-dimethylpyridine and CO), and the onset of activity was correlated with that of the formation of relatively strong Brønsted acid sites. The variation in the abundance of these sites correlated with the catalytic activity. Lewis sites were present but could not be directly associated with the activity. Raman, IR, and UV spectroscopy results indicated that the active sites were related to polymeric W surface species.

Introduction

A large number of industrially important reactions are catalyzed by solid acids. To improve their performance, a detailed characterization of these catalysts is important. Specifically, a systematic study of the development of acid sites in relation to the nature of the surface structure is of particular interest.

Supported metal oxides often show acidic properties and form an important "class" of solid acids. Thus, many such systems have been thoroughly investigated. However, the origin of the acidity, the development of the acid sites, and their relations with the surface species are not, to date, fully understood. WO_x supported on alumina[1−5] or titania[4−7] were extensively studied. Interest in tungstated zirconia increased since Arata and Hino showed that they could isomerize *n*-alkanes when prepared according to specific synthesis procedures.[8] Their catalytic behavior was studied for several reactions such as alcohol decomposition,[9−11] *n*-pentane[12,13] or *n*-butane[14] isomerization, *o*-xylene isomerization,[15] or alkane hydroisomerization in the presence of platinum.[16−18]

The above-mentioned studies were mostly performed on solids prepared by impregnating zirconium oxyhydroxide with a tungsten precursor followed by calcination at high temperature. Strong acid sites were created in this process.[8,13,14] Possible structures were proposed for the acid sites involving mainly 2D polymeric tungstate species.[14,19] Recent studies also indicated that a minimum surface density of W was required for any significant activity to develop.[12,15] However, drastic synthesis conditions adopted for such preparations lead to large modifications of the zirconia support with possible incorporation of the support into the structure of the deposited phase. This complicates attempts to establish a correlation between the surface structure and catalytic performance.

WO_x/ZrO_2 can also be obtained by impregnation of *zirconium oxide* followed by mild calcination conditions. In this case, the acid sites are thought to be weaker. However, results from our group indicated a catalytic behavior similar to that observed for tungstated zirconia prepared from zirconium oxyhydroxide (i.e., onset of activity after a minimum of W loading).[20,21] Clearly, it is of interest to investigate the development of acidity for the well-defined WO_x/ZrO_2 system (ex-monoclinic ZrO_2). Equally important for investigating the surface structure/activity relationship is restricting the studies to catalysts containing only surface W species (i.e., free of bulk WO_3).

Thus, the purpose of the present paper is (i) to obtain a series of WO_x/ZrO_2 catalysts where W is present as a surface phase at various coverages, (ii) to authenticate the molecular structure of the catalyst surface, (iii) to investigate the development of acidity as a function of coverage, and (iv) to assay the catalytic performance for an acid-catalyzed reaction. The ultimate objective is to seek a correlation between the activity, acidity, and molecular structure of the surface species. Toward this end, the solids were characterized by X-ray diffraction (XRD), Raman, Fourier transform infrared (FTIR), and UV spectroscopy, and a probe reaction.

Experimental Section

1. WO_x/ZrO_2 Catalyst Synthesis. WO_x/ZrO_2 samples were prepared by the adsorption of a W precursor on the surface of crystallized zirconia (ZrO_2). The zirconia support was prepared by the hydrolysis of zirconium *n*-propoxide [($Zr(OPr)_4$, 70% in propanol, Aldrich]. The precipitate thus obtained was washed free of propanol, dried at 393 K in air overnight, and calcined at 823 K in air for 24 h.[22]

A series of samples was prepared by the equilibrium adsorption method[23] by suspending a known amount of ZrO_2 in a large volume of aqueous ammonium metatungstate solution [$(NH_4)_6H_2W_{12}O_{40}$, Aldrich] 0.01 M (in metatungstate species) at a given pH from 2 to 12 and for a given time. After typically 96 h, the samples were filtered, washed with an aqueous solution at the same pH, dried overnight at 393 K in air, and finally calcined at 773 K in air for 24 h.

Samples will be designated as W*x* Z, where *x* refers to the surface density in W atoms/nm^2. W contents were measured

* To whom correspondence should be addressed. E-mail: marwan.houalla@ensicaen.fr.

10.1021/jp048435m CCC: $30.25
Published on Web 01/20/2005

by inductively coupled plasma-atomic emission spectrometry (ICP-AES).

2. BET Surface Area. Nitrogen adsorption was measured at 77 K with an automatic adsorptiometer (Micromeritics ASAP 2000). The samples were pretreated at 573 K for 2 h under vacuum. The surface areas were determined from adsorption values for five relative pressures (P/P_0) ranging from 0.05 to 0.2 using the Brunauer−Emmett−Teller (BET) method. The pore volumes were determined from the total amount of N_2 adsorbed between $P/P_0 = 0.05$ and $P/P_0 = 0.98$.

3. X-ray Diffraction. X-ray powder diffraction spectra were recorded using a Philips X'pert diffractometer with a copper anode ($K\alpha_1 = 0.154\ 05$ nm) and a scanning rate of $0.025°\cdot s^{-1}$. The results were used to estimate the relative amount of monoclinic and tetragonal zirconia. The intensities of the $(11\bar{1})$ and (111) reflections of the monoclinic phase and the (111) reflection of the tetragonal phase were used for quantification. The intensity ratio (X_m) was calculated using eq 1, and the fraction of monoclinic zirconia (V_m) was estimated from an empirical nonlinear relationship (eq 2).[24]

$$X_m = \frac{I_m(11\bar{1}) + I_m(111)}{I_m(11\bar{1}) + I_m(111) + I_t(111)} \quad (1)$$

$$V_m = \frac{1.31X_m}{1 + 0.31X_m} \quad (2)$$

4. Raman Spectroscopy. Raman characterization was performed on samples exposed to ambient conditions and following dehydration. The samples were dehydrated in a N_2-O_2 (75%−25%) flow at 723 K for 2 h. They were, then, transferred to the Raman cell, in a glovebox, under controlled atmosphere (N_2). Raman spectra were recorded with a FT-Raman instrument (Perkin-Elmer) equipped with a InGaAs laser source ($\lambda = 980$ nm). The spectra were acquired at 100 mW following 100 scans (resolution 4 cm^{-1}). No degradation of the sample was observed: a spectrum of the sample was recorded initially after only a few scans and compared with the final spectrum. In addition, hydrated samples did not show any peak due to dehydration (e.g., in the W═O region).

Raman results were used to measure the relative amount of monoclinic and tetragonal zirconia, to detect the eventual presence of WO_3 crystallites and to monitor the formation and evolution of W surface species. The percentage of the different phases of zirconia was determined from the intensity of the peaks characteristic of the monoclinic (178 and 189 cm^{-1}) and tetragonal (148 cm^{-1}) phases using a nonlinear relationship obtained by Kim et al.[25] from physical mixtures of monoclinic and tetragonal zirconia.

5. Infrared Spectroscopy. *Sample Preparation*. Samples were pressed into pellets (∼20 mg for a 2 cm^2 pellet) and activated at 723 K. Two methods were used for the activation:

For the experiments at room temperature or above (notably for the characterization of the structure of the catalysts or after adsorption of 2,6-dimethylpyridine), the samples were first heated under vacuum at 723 K for 1 h. This was followed by a treatment in O_2 ($P_{equilibrium} = 13.3$ kPa) for 1 h and evacuation for 1 h at 723 K before cooling down to room temperature (RT).

For the study of CO adsorption at low temperature, the samples were heated in an IR cell, in N_2 flow at 723 K for 2 h. The cell was cooled to 523 K, and nitrogen was allowed to flow for 3 h. The cell was then brought to the IR setup, closed under nitrogen, evacuated at RT, heated in O_2 ($P_{equilibrium} = 13.3$ kPa) at 623 K for 1 h, and evacuated for 1 h at 523 K before cooling to 77 K.

IR Measurements. IR spectra were recorded with a Nicolet 710 FTIR spectrometer (resolution 4 cm^{-1}, 128 scans). All the spectra presented here were normalized for 100 mg of the solid.

2,6-Dimethylpyridine (lutidine) was introduced at RT ($P_{equilibrium} = 133$ Pa), after activation. The spectra were then recorded following desorption from 323 to 573 K. The amount of Brønsted acid sites titrated by 2,6-dimethylpyridine was calculated using a molar extinction coefficient value of $\epsilon = 6.8$ $cm\cdot\mu mol^{-1}$ for both the ν_{8a} and ν_{8b} vibrations of protonated lutidine ($DMPH^+$) at ∼1644 and ∼1628 cm^{-1}.[26]

CO was introduced at 77 K in increasing amounts from 0.087 μmol to an equilibrium pressure of 133 Pa. In the ν(CO) region (2100−2200 cm^{-1}), the spectrum for a given solid was subtracted from that obtained following CO adsorption. When necessary, the contribution of CO in the gas phase was removed by subtraction of the gas-phase spectrum.

6. UV−Visible Spectroscopy. In the same procedure for Raman measurements, the samples were dehydrated in a N_2-O_2 (75%−25%) flow at 723 K for 2 h and then transferred to the UV cell in a glovebox under controlled atmosphere (N_2). A UV−visible source (Avantages) was directed toward the quartz cell via an optical fiber. Absorbance spectra were then transformed with the Kubelka−Munk function. The value of the absorption edge energy was determined for each spectrum by a linear extrapolation to zero absorption.

7. Catalytic Activity. The catalytic conversion of 2-propanol was measured in a fixed bed flow reactor. A 100 mg portion of the sample was pretreated at 723 K in N_2 for 2 h (ramp 5 $K\cdot min^{-1}$; 60 $mL\cdot min^{-1}$). The reaction was performed under atmospheric pressure with N_2 as the carrier gas ($P_{2-propanol} = 1.23$ kPa) at 403 and 413 K for various weight-hourly space velocities (WHSV) (8.7−53.3 $mmol\cdot h^{-1}\cdot g^{-1}$). Reactants and products were analyzed with an online gas chromatograph (HP 5890 Series II) equipped with a capillary column (CP WAX 52 CB) and a flame ionization detector (FID). No deactivation was observed, and polymerization products were never detected.

Results

1. W Adsorption. For supported catalysts prepared by the equilibrium adsorption method, the extent of adsorption by the support is a function of the solution concentration, the pH,[23] and the contact time. In the present study, the adsorption experiments were carried out using a W concentration of 0.01 $mol\cdot L^{-1}$ at pHs ranging from 2 to 12 for 96 h. For low W loadings, the solids were obtained by adsorption at pH 12 for periods from 1 to 96 h.

Figure 1a shows the variation of W uptake as a function of pH. In agreement with the results of Gazzoli et al.,[23] the amount of W adsorbed decreases with increasing solution pH. W uptakes were similar to those reported by Valigi et al.[27] For a given pH (pH 12), an initial steep increase in W uptake with adsorption time is observed, followed by a more progressive increase for longer adsorption periods (Figure 1b).

By varying the pH or the contact time, W loadings ranging from 1 to 4.6 wt % (0.9−3.5 W atoms/nm^2) were obtained. Table 1 reports the characteristics of the catalysts thus prepared. W surface densities were calculated on the basis of the surface area of the zirconia support considering that the latter was little affected by W deposition. Also reported in Table 1 is the nominal monolayer coverage assuming a theoretical monolayer value of 4.9 W atoms/nm^2.[28,29]

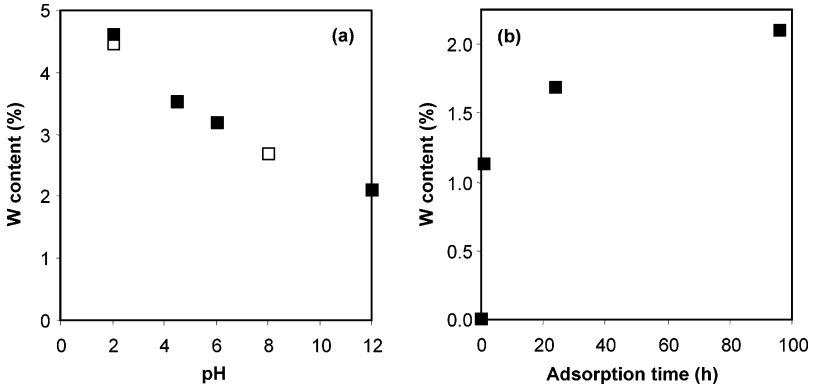

Figure 1. Preparation of WO_x/ZrO_2 catalysts: (a) (■) evolution of the amount of adsorbed W as a function of pH of the tungstate solution (adsorption time 96 h), (□) results calculated from Valigi et al;[27] (b) evolution of the amount of adsorbed W as a function of the adsorption time ($pH_{solution}$ 12).

TABLE 1: W Content and Some Characteristics of the WO_x/ZrO_2 Catalysts Obtained by Adsorption

sample name	ZrO_2	W0.9 Z	W1.3 Z	W1.6 Z	W2.4 Z	W2.7 Z	W3.5 Z
pH; adsorption time		12; 1 h	12; 24 h	12; 96 h	6; 96 h	4.5; 96 h	2; 96 h
surface area (m^2/g)	46	47	46	46	47	45	45
pore volume (cm^3/g)	0.18	0.18	0.19	0.19	0.19	0.18	0.19
wt % W	0	1.1	1.7	2.1	3.2	3.5	4.6
wt % WO_3	0	1.4	2.1	2.65	4.0	4.4	5.8
W atoms/nm^2	0	0.9	1.3	1.6	2.4	2.7	3.5
% of monolayer[a]	0	18	27	33	49	55	71
% monoclinic phase	93	96	94	96	94	95	95

[a] Assuming a theoretical monolayer for 4.9 W atoms/nm^2.

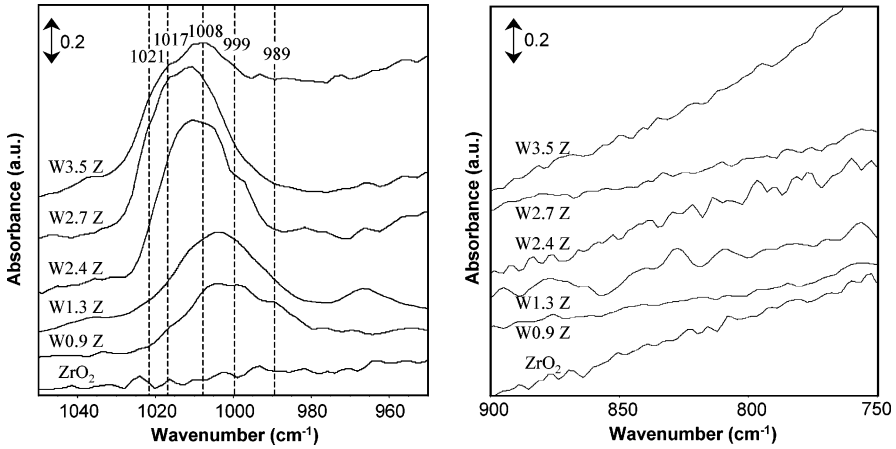

Figure 2. Raman spectra of zirconia and WO_x/ZrO_2 catalysts pretreated in dry air at 723 K.

2. X-ray Diffraction. The XRD patterns of the zirconia support showed intense peaks for $2\theta = 28.2°$ ($d = 3.16$ Å) and 31.5° ($d = 2.83$ Å) and a weak one at 30.2° ($d = 2.95$ Å). The first two peaks are characteristic of the $(11\bar{1})$ and (111) planes of the monoclinic phase. The peak at 30.2° corresponds to the (111) plane of the tetragonal phase.[14,18] From the relative intensities of these peaks, it was estimated that zirconia was essentially present in the monoclinic form (93%). The W content had no significant effect on the composition (Table 1). XRD patterns showed no additional peaks which can be attributed to bulk WO_3 (characteristic peaks at $2\theta = 23.1$, 23.6, and 24.4°;[14] $d = 3.84$, 3.77, and 3.65 Å, respectively).

3. Raman Spectroscopy. Raman spectra of the solids were first recorded at room temperature under ambient conditions. The vibrations characteristic of zirconia appear mainly in the region between 100 and 700 cm^{-1}. The zirconia support showed the expected peaks for monoclinic[24,25] (peaks at 178, 189, and 476 cm^{-1}) and tetragonal zirconia phases (peaks at 146, 267, and 459 cm^{-1}). Consistent with XRD data, the intensity of these peaks was not significantly affected by W deposition, indicating that the composition of the zirconia phase was not modified.

Although bulk WO_3 can be easily detected by Raman spectroscopy because of its high scattering cross section, no peaks characteristic of WO_3 (bands at ~806 and ~713 cm^{-1})[14,29] were observed for all catalysts. In addition to the peaks attributed to the support, the Raman spectra for W-containing catalysts exhibited a single new band in the 935−965 cm^{-1} region. The position of the band shifts from 935 to 965 cm^{-1} with increasing W content. This band was attributed to the stretching vibration of the W═O monooxo species.[23,24,29−32] Since catalysts are dehydrated prior to catalytic experiments, Raman spectra were also recorded following in situ calcinations of the solids. As expected, upon dehydration, the band described above shifted to a higher wavenumber.[3,5] Figure 2 shows the 1050−950 and 900−750 cm^{-1} regions of the Raman spectra for zirconia and WO_x/ZrO_2 after dehydration at 723 K. For dehydrated solids,

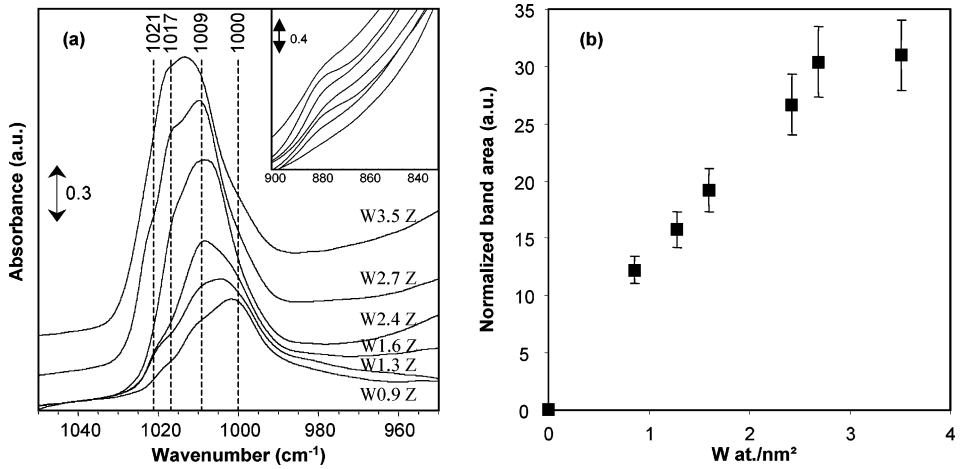

Figure 3. (a) Infrared spectra for zirconia and WO_x/ZrO_2 catalysts activated in a vacuum at 723 K (spectrum of ZrO_2 subtracted). The inset shows the same spectra in the region 800−900 cm^{-1}. (b) Evolution of the W═O band area (measured between 970 and 1035 cm^{-1}; normalized to 100 mg) with W density.

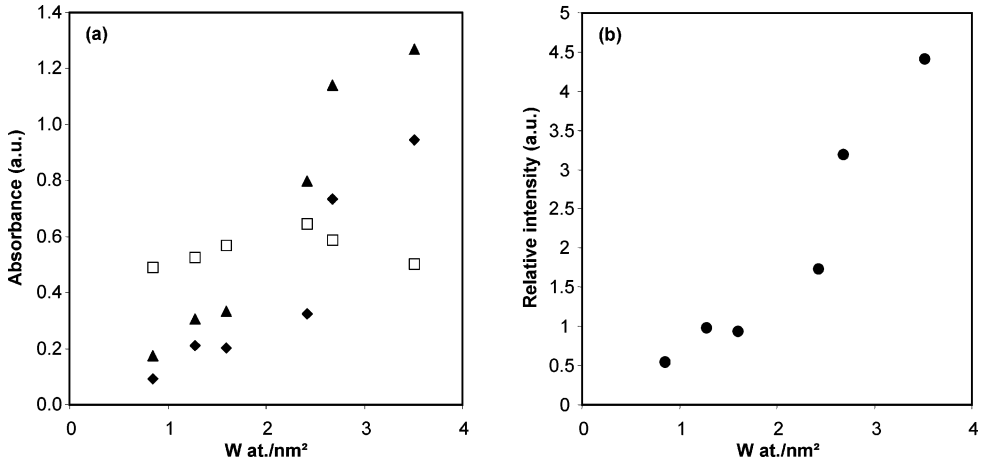

Figure 4. Evolution of the IR ν(W═O) band for WO_x/ZrO_2: (a) peak at 1021 cm^{-1} (◆), 1017 cm^{-1} (▲), and 1000 cm^{-1} (□) (normalized to 100 mg); (b) relative intensity $(I_{1021} + I_{1017})/I_{1000}$.

the maximum of the W═O band is shifted from 1000 to 1012 cm^{-1} with W content. Depending on the solid, several peaks or shoulders may be seen at 989, 999, 1008, 1017, and 1021 cm^{-1}. The contribution of the high wavenumber bands appears to increase with the W loading. However, due to the low signal-to-noise ratio, the actual presence of peaks at these positions may not be fully ascertained. Bands attributed to W−O−W in the region 830−880 cm^{-1} were not detected for all catalysts (Figure 2).

4. IR Spectroscopy. *4.1. Structure.* IR spectroscopy was used to characterize the structure of the dehydrated solids and to evaluate their acidity. Figure 3a shows the IR spectra of WO_x/ZrO_2 catalysts in the region of (W═O) vibrations following dehydration treatment. A broad band centered around 990 cm^{-1} observed in the hydrated solids shifted to higher wavenumbers (1000−1020 cm^{-1}) upon calcination. A weak band, detected at 880 cm^{-1} (Figure 3a, inset), was attributed to W−O−W vibration.[31] The intensity of this band appears to increase with W content. The band at 1000−1020 cm^{-1} is attributed to W═O stretching vibrations.[12,24,30] The total area of the band increased with W surface density until it reached an apparent plateau for high W content (Figure 3b). For low W loading, the maximum of the band was centered at 1002 cm^{-1}. It shifted progressively to 1014 cm^{-1} with W loading. A close inspection of the spectra shows that the W═O band consisted of several peaks or shoulders at 1021, 1017, 1009, and 1000 cm^{-1} similar, in position, to those observed by Raman spectroscopy at 1021, 1017, 1008, and 999 cm^{-1}. The same peaks or shoulders were observed regardless of the activation mode of the catalysts (in nitrogen flow or in a vacuum).

The intensity of the peaks at 1021,1017, and 1000 cm^{-1} was monitored as a function of W content. The observed variation may be considered, in a first approximation, as indicative of the evolution of the components of the W═O band. (Figure 4a). Note that the intensities of the peaks at high wavenumbers (I_{1021} and I_{1017}) increase with the W content, whereas that of the low wavenumber peak at 1000 cm^{-1} does not evolve significantly with W loading. Figure 4b shows that the relative intensity $(I_{1021} + I_{1017})/I_{1000}$ increases slightly up to 1.6 W atoms/nm^2. This is followed by a faster increase for higher W content. Similar results were obtained after curve fitting.

4.2. Acidity. 4.2.1. Lutidine Adsorption. 2,6-Dimethylpyridine (lutidine) is known to be a more sensitive probe of Brønsted acid sites than pyridine due to its higher basicity and to the steric hindrance of the methyl groups.[26,33,34] Figure 5a shows the IR spectra of lutidine adsorbed on zirconia and tungsten supported on zirconia between 1680 and 1590 cm^{-1}. This region is characteristic of the ν_{8a} and ν_{8b} vibrations of 2,6-dimethylpyridine coordinated to a Lewis acid site (bands at ∼1610 and ∼1580 cm^{-1}), protonated on a Brønsted acid site (bands at ∼1643 and ∼1628 cm^{-1}), or interacting weakly through a hydrogen bond (1590 cm^{-1}).[33,34] In agreement with the literature,[22,34] the adsorption of lutidine on zirconia gave rise to bands at 1580 and 1610 cm^{-1} characteristic of Lewis acid sites. No

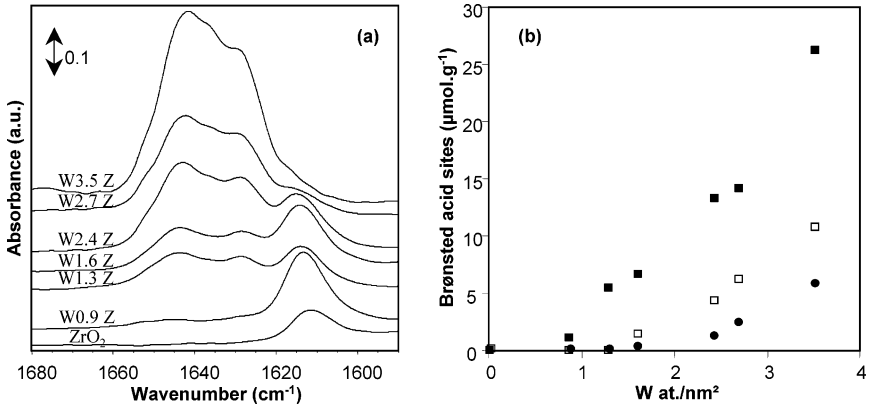

Figure 5. Lutidine adsorption followed by IR spectroscopy: (a) IR spectra for ZrO_2 and WO_x/ZrO_2 catalysts after lutidine desorption at 423 K; (b) evolution of the concentration of Brønsted acid sites for ZrO_2 and WO_x/ZrO_2 catalysts following lutidine desorption at 423 K (■), 523 K (□), and 573 K (●).

Brønsted acid sites were detected. For WO_x/ZrO_2, a doublet appeared at 1644 and 1629 cm^{-1} attributed to lutidinium ions. The positions of the peaks were similar for all catalysts, but their intensity increased with W content. Figure 5b shows the evolution of the concentration of Brønsted acid sites following desorption at 423, 523, and 573 K for various catalysts. Following desorption at 523 or 573 K, a threshold of W content is observed for the formation of Brønsted acid sites. Below 1.3 W atoms/nm^2, WO_x/ZrO_2 did not exhibit Brønsted acid sites strong enough to retain the probe molecule at these temperatures. For higher loadings, Brønsted acid sites were observed. Their concentration increases with W loading up to 10.9 μmol of $H^+ \cdot g^{-1}$ at 523 K and 5.9 μmol of $H^+ \cdot g^{-1}$ at 573 K. Desorption at 423 K showed a similar tendency. However, lower desorption temperatures reveal a larger abundance of Brønsted acid sites and a lower threshold for their formation. The sites detected at 423 K were weakly acidic, as they readily disappear upon heating.

4.2.2. CO Adsorption. Carbon monoxide is a weak base. At a low temperature (77 K), it can form coordination bonds with Lewis acid sites and hydrogen bonds with surface hydroxyls.[35,36] This probe also provides additional information on the strength of the Brønsted acid sites of the solids. When hydrogen bonds are formed between CO and the hydroxyls, the ν(CO) vibration is shifted toward higher wavenumbers, while ν(OH) is shifted toward lower wavenumbers. For both vibrations, a larger shift reflects a stronger acid site.[37]

The IR spectrum for zirconia under an equilibrium pressure of 133 Pa CO at 77 K (Figure 6) exhibits three main bands at 2183, 2169, and 2149 cm^{-1} and two shoulders at 2160 and 2138 cm^{-1}. The bands at 2183 and 2169 cm^{-1} are attributed to CO adsorbed on Lewis acid sites.[34,35,38,39] The bands at 2160 and 2149 cm^{-1} are due to CO interacting with Brønsted acid sites,[34,38] and the shoulder at 2139 cm^{-1} is due to physisorbed CO. The latter band due to physisorbed CO at 2139−2143 cm^{-1} was barely detected for zirconia and for low W loadings but becomes prominent for high W content. The amount of CO adsorbed on Lewis acid sites decreased strongly with W loading. With increasing W content, the spectra for WO_x/ZrO_2 catalysts showed that the bands due to Lewis sites shifted from 2175 to ∼2200 cm^{-1} and those due to Brønsted acid sites shifted from 2156 to 2164 cm^{-1}. In both cases, the shift increases with W content, indicating an increase in acid strength.

When only a small dose of CO was adsorbed on the surface (Figure 7), the band due to physisorbed CO at 2139−2143 cm^{-1} was no longer detected, indicating that the admitted amount (0.29 μmol of CO) was essentially adsorbed. The position of

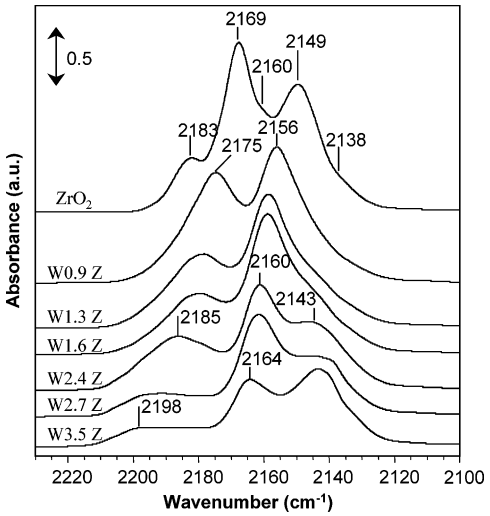

Figure 6. IR spectra for ZrO_2 and WO_x/ZrO_2 under an equilibrium pressure of 133 Pa CO at 77 K. (The spectra were obtained after subtraction of the spectrum of the solid after activation in a vacuum and the gas-phase spectrum.)

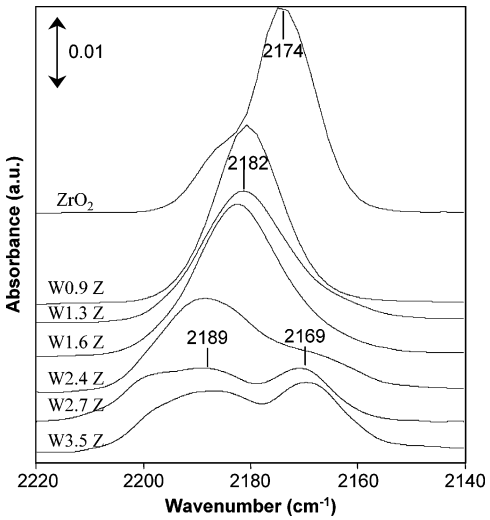

Figure 7. IR spectra for ZrO_2 and WO_x/ZrO_2 after adsorption of 0.29 μmol of CO at 77 K. (The spectra were obtained after subtraction of the spectrum after activation in a vacuum.)

the remaining peaks, compared to that in Figure 6, shifted toward higher wavenumbers, suggesting that the strongest acid sites are detected first. Solids with low W loadings showed essentially one main band around 2182 cm^{-1} characteristic of Lewis acid

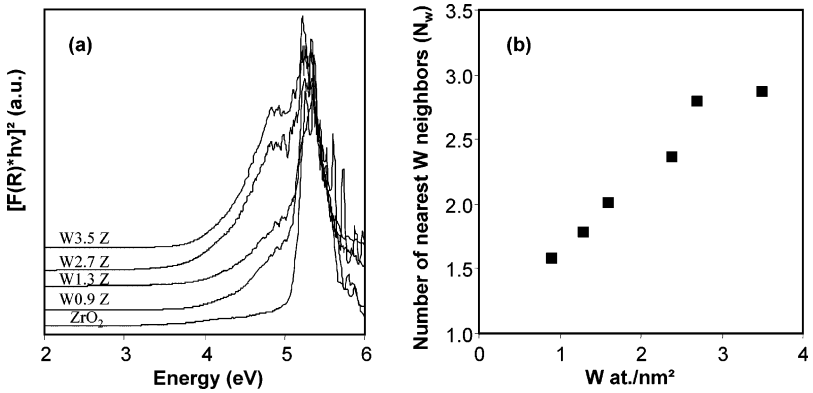

Figure 8. (a) UV−visible spectra for ZrO_2 and WO_x/ZrO_2 catalysts after activation in air at 723 K; (b) number of nearest W neighbors for WO_x/ZrO_2 catalysts vs W density.

TABLE 2: Evolution of the Absorption Edge Energy of WO_x/ZrO_2 Samples

sample	W0.9 Z	W1.3 Z	W1.6 Z	W2.4 Z	W2.7 Z	W3.5 Z
Eg (eV)	4.23	4.15	4.06	3.92	3.75	3.72
no. of nearest W neighbors (N_w)	1.6	1.8	2.0	2.35	2.8	2.9

sites. The spectra for solids containing more than 1.6 W atoms/nm^2 exhibited a band at 2169 cm^{-1} which corresponds to strong Brønsted acid sites. Although one cannot preclude the presence of this band for solids containing a low W loading, the results appear to indicate its presence only above 1.6 W atoms/nm^2. Similar behavior was observed after curve fitting the IR spectra for solids under an equilibrium pressure of 133 Pa CO. This suggests that, in accordance with the results obtained with lutidine, a minimum of W loading is required for the appearance of strong Brønsted acid sites.

5. UV Spectroscopy. Previous studies by Fournier et al.[40] indicated that the position and width of the UV absorption band for polyoxomolybdate ions are a function of the degree of condensation of these species. Weber[41] showed a linear correlation between the value of the absorption edge energy (Eg) for reference molybdenum-based solids and the number of Mo nearest neighbors in these compounds. This methodology was used by several authors to follow the evolution of the size of WO_x domains.[16,19,23,24,42]

UV−visible spectra for ammonium metatungstate and crystalline WO_3 indicate that the absorption edge energies of these compounds are respectively 3.3 and 2.9 eV, in agreement with the literature.[16,19,42] The absorption edge energy for sodium tungstate was reported to be equal to 4.9 eV.[19] The number of next nearest neighbors for WO_3, $(NH_4)_6W_{12}O_{40}$, and Na_2WO_4 is respectively 6, 4, and 0. With these reference compounds, the following linear relationship can be obtained between the absorption edge energy (Eg) and the number of nearest tungsten neighbors (N_w):

$$N_w = -2.87\mathrm{Eg} + 13.93 \quad (3)$$

Figure 8a shows the UV−visible spectra for zirconia and WO_x/ZrO_2 catalysts after activation at 723 K in air. As expected,[19,24,30] the spectra for the zirconia support exhibited an absorption edge energy of 5.1 eV, characteristic of the charge transfer $O^{2-} \rightarrow Zr^{4+}$. The absorption edge energy for tungstate species in WO_x/ZrO_2 spectra decreases from Eg = 4.23 eV for W0.9 Z to Eg = 3.72 eV for W3.5 Z catalyst (Table 2). From Eg, using eq 3, the number of nearest tungsten neighbors (N_w) was calculated for all tungsten-supported samples (Table 2). Figure 8b shows the evolution of N_w versus the W density. N_w increases from 1.6 for the lowest W content to 2.9 at 3.5 W atoms/nm^2 where it appears to level off.

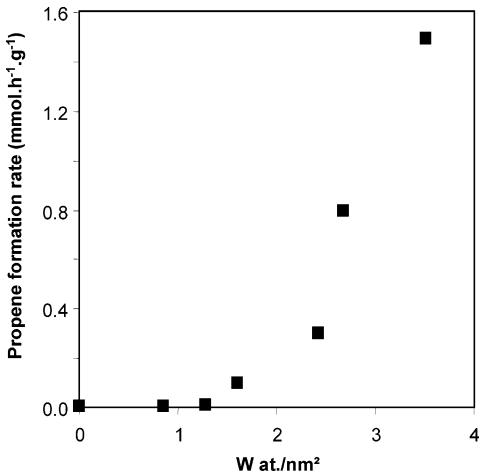

Figure 9. Propene formation rate as a function of W surface density in WO_x/ZrO_2 catalysts. Reaction temperature, 403 K; molar space velocity, 35.5 mmol of propanol·h^{-1}·g^{-1}.

6. Catalytic Activity Measurements. 2-Propanol decomposition is a well-established model reaction for monitoring the acidity of solids.[43−47] Dehydration reportedly occurs on Lewis or Brønsted acid sites, leading to propene and diisopropyl ether formation, whereas dehydrogenation takes place on basic or redox sites, yielding acetone.[43,44,46,48,49] The rate of propene formation has been related to the acidity of the catalyst as monitored by several adsorption/desorption methods.[22,44]

At 413 K, the propene formation rate was not affected by 2-propanol pressure in the 0.38−2.75 kPa range. This indicates zero-order kinetics with respect to the reactants, in agreement with earlier reports.[44,45] Under the conditions used in the present study (403 or 413 K, 60 or 120 mL·min^{-1} flow), the zirconia support was not active. With active WO_x/ZrO_2, propene and diisopropyl ether were formed but acetone was not detected. For all W contents, the selectivity to propene exceeded 85%.

The propene formation rate is plotted in Figure 9 versus the W surface density. The same trend was observed for different reaction temperatures (403 → 423 K) or 2-propanol molar space velocities (8.9 → 53.3 mmol·h^{-1}·g^{-1}). A minimum of W density was required for the appearance of catalytic activity: solids with a W density below 1.3 W atoms/nm^2 were totally inactive; for higher W densities, the activity increased progressively with W loading up to 1.5 mmol·h^{-1}·g^{-1} for W3.5 Z.

Discussion

Catalyst Preparation. The results of catalyst preparation by equilibrium adsorption indicate that it is possible to obtain a series of WO_x/ZrO_2 containing up to 3.5 W atoms/nm^2 by varying the pH of the adsorption solution. The observed decrease of W uptake with increasing pH can be qualitatively related to the point of zero charge (PZC) of the support. For pHs lower than the PZC of the support (4.5−6.7 for zirconia[23]), a positive charge will develop at the surface which favors electrostatic interactions with negatively charged tungstate species in solution (WO_4^{2-}, $W_7O_{24}^{6-}$, $H_2W_{12}O_{40}^{6-}$, and $H_2W_{12}O_{42}^{10-}$).[23,51] Conversely, for pHs higher than the PZC of the support, the surface becomes negatively charged, inhibiting the adsorption of W anions.[52] A close inspection of the results indicates, however, that a model solely based on electrostatic interactions cannot entirely explain the observed behavior. For instance, at a pH of 12, the surface must be negatively charged and should not favor the adsorption of W anionic species.[23,51,52] The observed uptake of 1.6 W atoms/nm^2 of zirconia under these unfavorable conditions can be attributed to the anchoring of W species by chemical reactions with surface hydroxyls.[52,53]

BET, XRD, and Raman spectroscopy (under ambient conditions) indicated that this preparation method did not affect the specific surface area and the composition of the support (monoclinic−tetragonal distribution). Furthermore, in agreement with the findings reported by Gazzoli et al.,[23] the results clearly show that the preparation method precludes WO_3 formation.

Structure of Surface W Species. The absence of the Raman peaks characteristic of WO_3 and the presence of the peak at ∼1010 cm^{-1} (Figure 2) indicate, as suggested earlier,[4,19,31,54] that the supported phase is present as a surface W species.

The molecular structure of the surface W phase has been the subject of detailed investigation by Wachs and co-workers.[32] Their results indicated the presence of monooxo-tungstate species. Previous studies of WO_x/ZrO_2 obtained by the impregnation of crystallized ZrO_2 reported the presence of a single Raman peak.[4] This is in variance with our IR results which show the presence of several peaks or shoulders at ∼1021, ∼1017, ∼1009, and ∼1000 cm^{-1}. Similar indications, although less conclusive, were obtained from Raman spectra. Consistent with this finding are the IR results of Gutiérrez-Alejandre et al.,[30] which show the presence of a peak at 1002 cm^{-1} and two shoulders at 1012 and 1005 cm^{-1}. The existence of several bands attributed to M (Mo or V)═O has also been reported for the corresponding MoO_x/ZrO_2[9,55] and VO_x/ZrO_2[56] systems.

It is interesting to note that the results reported in the present study for WO_x/ZrO_2 catalysts prepared by the impregnation of *monoclinic ZrO_2* are in accord with those reported for systems obtained by the *impregnation of Zr(OH)$_4$* followed by high temperature calcination. Indeed, Scheithauer et al.[24] reported, for tungstated zirconia catalysts (ex $Zr(OH)_4$) calcined at 923 K, infrared bands at 1017−21, 1008−14, and 995 cm^{-1} depending on the W content. Infrared spectra of the solids following calcination at 1098 K showed bands at 1021−24, 1013−15, 1005−06, and 997 cm^{-1}.[12] Under the same conditions, Raman results revealed the presence of two peaks at 1021−22 and 1000 cm^{-1}.[24]

The presence of several Raman or IR W═O stretching bands was attributed by Scheithauer et al.[24] to the existence of different W species. For the WO_x/TiO_2 system, Eibl et al.[54] attributed the presence of several Raman and infrared bands characteristic of ν(W═O) to a different degree of polymerization of W species. A similar hypothesis has been proposed by Afanasiev et al.[9] and Prinetto et al.[55] to account for the observed Raman and IR bands characteristic of ν(Mo═O). Bands at low wavenumbers were ascribed to monomeric Mo species, whereas high wavenumber peaks were attributed to the extensive polymerization of Mo species. These results were consistent with a shift of ν(metal═O) of the aqueous complexes of tungsten[57] or molybdenum[55] toward higher wavenumbers with the degree of condensation. Thus, from the literature data concerning the WO_x/ZrO_2, WO_x/TiO_2, and MoO_x/ZrO_2 systems, it is reasonable to assume that the existence of several bands characteristic of ν(W═O) reflects the presence of different degrees of condensation of W species. The shift to high wavenumber suggests an increased extent of polymerization of W species with increasing W loading. This hypothesis is consistent with UV−visible results which show a decrease in the energy threshold for absorption (Table 2) and thus an increase of the number of W nearest neighbors with increased loading. It is also in agreement with earlier Raman studies indicating the presence of polytungstate species for high loading.[4,24] However, in variance with the results of Scheithauer et al.,[24] Raman bands characteristic of polymeric species ν(W−O−W) were not detected in the present study. This may be tentatively attributed to the low signal-to-noise ratio observed here and the low Raman scattering cross section for such vibrations compared to that of W═O.[30] By contrast, it is noteworthy that a band attributed to ν(W−O−W) was observed in the IR spectra.

Acidity of Surface Species. *(a) Lewis Acidity.* The low temperature CO adsorption results indicate a significant decrease in the total number of Lewis acid sites with increasing loading (i.e., increasing nominal coverage of the support) (Figure 6). This is in accord with early results[12,58,59] and was ascribed to a blocking of coordinatively unsaturated Zr^{4+} (Lewis acid sites) by the supported W phase.[12,59] The enhanced Lewis acidity of zirconia upon deposition of the WO_x phase indicated in the present study was observed for tungstated zirconia catalysts (ex $Zr(OH)_4$)[12,24] and attributed to inductive effects of neighboring WO_x species.[24]

(b) Brønsted Acidity. The evolution of Brønsted acidity with W loading was monitored by the adsorption of lutidine and CO probe molecules, followed by infrared spectroscopy.

The lutidine adsorption results indicated that a minimum of W loading is required for the formation of strong Brønsted acid sites (sites which retain lutidine after thermodesorption at 573 K). No protonated lutidine species were detected for loadings lower than 1.3 W atoms/nm^2. For higher loadings, the abundance of Brønsted acid sites increased progressively with W loading. Low temperature CO adsorption data also suggest the presence of a threshold of W loading for the formation of strong Brønsted acid sites, illustrated by the appearance of a CO band at 2169 cm^{-1} following the adsorption of a small CO dose. This band was only detected for solids containing W loadings higher than 1.6 W atoms/nm^2.

To the best of our knowledge, the presence of a threshold of W loading for the appearance of Brønsted acid sites has not been reported, to date, for WO_x/ZrO_2 catalysts obtained by deposition on a monoclinic zirconia. However, indications for the occurrence of such behavior have been noted for tungstated zirconias obtained by the impregnation of zirconium oxyhydroxide. For instance, on the basis of pyridine adsorption measurements, Naito et al.[58] reported the presence and development of Brønsted acid sites for W contents higher than 3 W atoms/nm^2. Baertsch et al.[60] reported an increase in the abundance of Brønsted acid sites with increasing W loading. However, low loading catalysts were not examined; thus, the

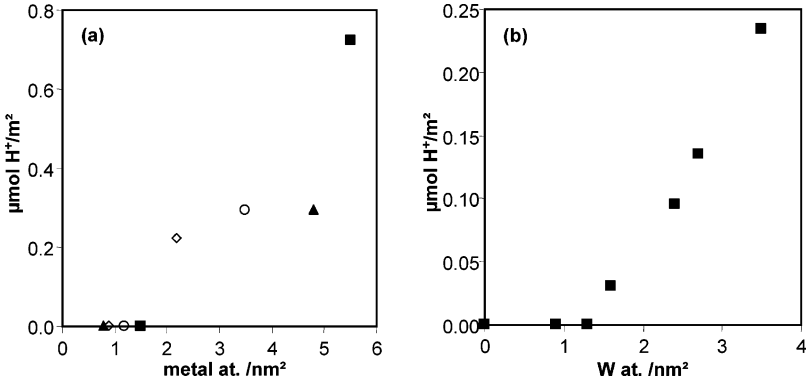

Figure 10. (a) Evolution of the abundance of Brønsted acid sites (determined by pyridine adsorption) for alumina-supported VO_x (■), NbO_x (▲), MoO_x (○), and ReO_x (◇) catalysts vs metal loading (results from Wachs and co-workers[31,63]); (b) evolution of the abundance of Brønsted acid sites (determined by lutidine adsorption) for WO_x supported on ZrO_2 catalysts vs W loading (present study).

existence of a threshold for the appearance of Brønsted acid sites cannot be ascertained.

It is of interest to compare the behavior of WO_x/ZrO_2 catalysts obtained by the impregnation of a zirconia with that of alumina-supported catalysts. Wachs and co-workers have examined the evolution of Brønsted acidity as monitored by pyridine for a series of alumina-supported MoO_x, ReO_x, VO_x, and NbO_x catalysts.[31,63] The results are reported in Figure 10a. Clearly, all alumina-supported systems exhibit a behavior similar to that observed for the WO_x/ZrO_2 catalysts (Figure 10b). Namely, for all the supported phases examined, a minimum of the surface density of the supported phase was required for the formation of Brønsted acid sites. A similar finding was recently reported for the NbO_x/ZrO_2 system.[61]

Activity Measurements. As observed for the evolution of the abundance of Brønsted acid sites with W content, activity data (Figure 9) clearly indicate that, for the catalysts to develop any meaningful activity, a minimum of W loading is needed. Catalysts containing up to 1.3 W atoms/nm^2 did not exhibit any activity for the reaction of 2-propanol decomposition. The activity is "turned on" for higher loadings and increases with increasing W content. This is in agreement with the results obtained by Vaidyanathan[20] for catalysts obtained by incipient wetness impregnation.

The catalytic behavior of WO_x/ZrO_2 catalysts obtained by the impregnation of a zirconia was compared to that for tungstated zirconia. For a similar type of reaction (dehydration of butanol), an increased activity with increasing W content between 2.9 and 6.8 W atoms/nm^2 was observed. However, because of the high W loadings used, the presence of a threshold could not be evidenced.[11] Note that the existence of such a threshold was clearly shown for other acid-catalyzed reactions (isomerization of *o*-xylene,[15] *n*-pentane,[12] and *n*-butane[62]).

Correlation between Acidity and Catalytic Performances. Figure 11 shows the variation of the rate of propene formation as a function of W content. Also shown in this figure is the abundance of Brønsted acid sites estimated from lutidine desorption at 573 K. The results clearly indicate a direct correlation between the catalytic activity and the presence and concentration of relatively strong Brønsted acid sites. For low W content ($\leq$1.3 W atoms/nm^2), catalysts show little activity and exhibit no Brønsted acidity. For higher W loadings, one can observe the simultaneous appearance of 2-propanol decomposition activity and Brønsted acid sites and a parallel evolution of these two parameters. The development of the CO band at 2169 cm^{-1} might also coincide with the onset of the activity.

For tungstated zirconia, prepared from zirconium oxyhydroxide, and for a similar type of reaction, namely, 2-butanol dehydration, a direct relationship between the abundance of Brønsted acid sites and the rate for 2-butanol dehydration was reported by Baertsch et al.[11] However, in this instance, Brønsted acid sites were reportedly created by the partial reduction of WO_x clusters with the reactant 2-butanol followed by a stabilization of the protons by the same clusters. This is in variance with our results where Brønsted acid sites were presumably present prior to the reaction. One possible way to reconciliate these findings is to assume that WO_x species associated with Brønsted acidity titrated by the adsorption of probe molecules prior to exposure to the reactants were directly related to those formed by reduction with the reactants.

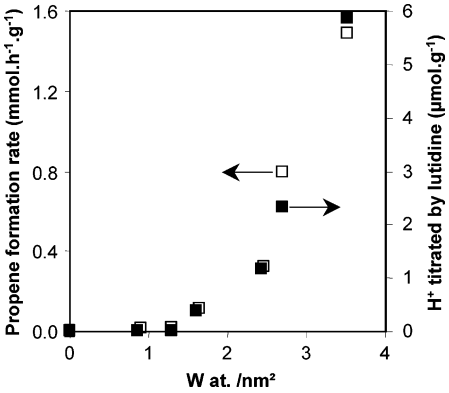

Figure 11. Correlation for WO_x/ZrO_2 catalysts between the abundance of Brønsted acid sites, determined by lutidine adsorption and desorption at 573 K (■), and the propene formation rate (□).

Correlation between the Nature of Surface W Species and Brønsted Acid Sites. Figure 12 compares the abundance of Brønsted acid sites estimated from lutidine desorption at 573 K with the variation of the intensity of both bands at 1021 and 1017 cm^{-1} atributed to ν(W═O) for polymeric species, both as a function of W content. Note the parallel behavior of these two parameters: catalysts which show little Brønsted acidity exhibit weak bands at 1021 and 1017 cm^{-1}. The sharp development of these bands for catalysts containing more than 1.6 W atoms/nm^2 coincides with the appearance and evolution of Brønsted acid sites.

Comparison between W Supported on Monoclinic Zirconia and Tungstated Zirconia. It will be of interest to compare the behavior of WO_x/ZrO_2 catalysts used in the present study and obtained by the deposition of W on essentially monoclinic *zirconium oxid*e with that reported for tungstated zirconia, *prepared from zirconium oxyhydroxide*. Although direct comparisons by the same authors were seldom made, the

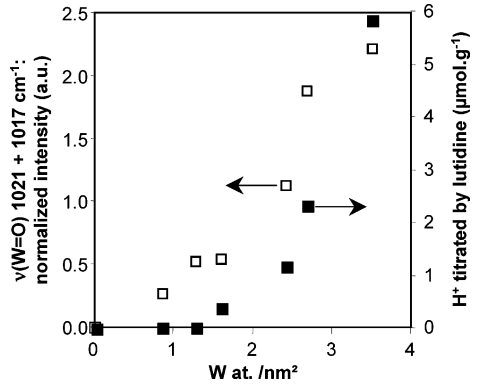

Figure 12. Correlation for WO_x/ZrO_2 catalysts between the abundance of Brønsted acid sites, determined by lutidine adsorption and desorption at 573 K (■), and the evolution of the sum of the intensities of ν(W═O) at 1021 and 1017 cm^{-1} (normalized to 100 mg) (□).

latter system was claimed to be more acidic than that synthesized from monoclinic zirconia.[8]

For both systems, the creation and development of Brønsted acid sites and activity for acid-catalyzed reaction occurred upon W addition. For both types of preparations, a threshold in metal content for the onset of activity was evidenced. Similarly, in both instances, a minimum amount of W was required for the appearance of Brønsted acidity. Common features were also noted in the analysis of the surface structure of the supported phase. Specifically, similar infrared and Raman bands characteristic of W═O vibrations were observed, indicating the presence, in both systems, of at least two W species of similar structures.

One possible interpretation for the similarity in the behavior of both systems is related to the type of preparation method used in the present study. Adsorption involves contacting the support, for an extended period of time, with a solution containing the precursor metal. Under these conditions, a partial formation of surface zirconium oxyhydroxide can be envisaged. Thus, the W phase will be deposited on a surface similar to that used for the synthesis of tungstated zirconia. However, comparable behavior for the activity, acidity, and surface structure was observed with solids obtained by the incipient wetness impregnation of titania.[64] This would imply that the reported difference in acidity (and activity) between solids prepared from zirconia and those obtained from zirconium oxyhydroxide, *if verified*, probably concerns a limited number of species, whereas most of the superficial species and acidic sites are similar. One type of species that will be, in principle, favored during the synthesis of tungstated zirconia which involves a more intimate interaction between the support and the W phase followed by a high temperature calcination is Zr-containing heteropolytungstate. The formation of such species has been indeed proposed by Scheithauer et al.[12] as being responsible for the creation of strong Brønsted acidity. A new type of dimeric Zr-containing polyoxotungstate was recently synthesized.[65] The study of its catalytic behavior and deposition on a support could help to determine the actual role of these species in the overall characteristics of tungstated zirconias.

Conclusions

A series of WO_x/ZrO_2 catalysts containing between 0.9 and 3.5 W atoms/nm^2 was prepared by the equilibrium adsorption method. XRD and Raman spectroscopy results indicated that the W phase is present as a surface interaction species. No evidence for the formation of WO_3 was found.

The molecular structure of the catalysts was examined by in situ Raman, infrared, and UV−vis spectroscopy. The results were interpreted in terms of the increased polymerization of W surface species with increasing W loading.

The evolution of the acidity upon W deposition was monitored by the adsorption of lutidine and CO followed by infrared spectroscopy. The results indicated the presence of a threshold of W loading (~1.6 W atoms/nm^2) for the appearance of relatively strong Brønsted acid sites. For higher loadings, a progressive increase in the abundance of these sites with W content is observed. Analysis of the catalytic activity for 2-propanol decomposition revealed similar behavior. Namely, a minimum of W loading was required before any significant activity could be observed.

A direct correlation was observed between the abundance of Brønsted acid sites and 2-propanol decomposition activity. From the comparison of these results with the molecular structure of the supported phase, one can infer that these sites are associated with polymeric W species characterized by ν(W═O) bands at 1021 and 1017 cm^{-1}.

Acknowledgment. The Van Gogh exchange Program is gratefully acknowledged for a grant. We thank Prof. B. M. Weckhuysen and Dr. T. Visser (Department of Inorganic Chemistry and Catalysis, University of Utrecht, The Netherlands) for making available the Raman and UV spectrometers and for their advice. Thanks are also due to Mrs. M. N. Metzner (Lab. SIFCOM, UMR CNRS 6176, ENSICAEN-Université de Caen) for performing the XRD measurements.

References and Notes

(1) Meijers, S.; Gielgens, L. H.; Ponec, V. *J. Catal*. **1995**, *156*, 147.
(2) Soled, S. L.; McVicker, G. B.; Murrell, L. L.; Sherman, L. G.; Dispenziere, N. C., Jr.; Hsu, S. L.; Waldman, D. *J. Catal*. **1988**, *111*, 286.
(3) Vuurman, M. A.; Wachs, I. E. *J. Phys. Chem*. **1992**, *96*, 5008.
(4) Kim, D. S.; Ostromecki, M.; Wachs, I. E. *J. Mol. Catal. A* **1996**, *106*, 93.
(5) Chan, S. S.; Wachs, I. E.; Murrell, L. L.; Wang, L.; Hall, W. K. *J. Phys. Chem*. **1984**, *88*, 5831.
(6) Engweiler, J.; Harf, J.; Baiker, A. *J. Catal*. **1996**, *159*, 259.
(7) Ramis, G.; Busca, G.; Cristiani, C.; Lietti, L.; Forzatti, P.; Bregani, F. *Langmuir* **1992**, *8*, 1744.
(8) Hino, M.; Arata, K. *J. Chem. Soc., Chem. Commun*. **1988**, 1259.
(9) Afanasiev, P.; Geantet, C.; Breysse, M.; Coudurier, G.; Vedrine, J. C. *J. Chem. Soc., Faraday Trans*. **1994**, *90*, 193.
(10) Larsen, G.; Lotero, E.; Petkovic, L. M.; Shobe, D. S. *J. Catal*. **1997**, *169*, 67.
(11) Baertsch, C. D.; Komala, K. T.; Chua, Y.-H.; Iglesia, E. *J. Catal*. **2002**, *205*, 44.
(12) Scheithauer, M.; Cheung, T.-K.; Jentoft, R. E.; Grasselli, R. K.; Gates, B. C.; Knözinger, H. *J. Catal*. **1998**, *180*, 1.
(13) Santiesteban, J. G.; Vartuli, J. C.; Han, S.; Bastian, R. D.; Chang, C. D. *J. Catal*. **1997**, *168*, 431.
(14) Boyse, R. A.; Ko, E. I. *J. Catal*. **1997**, *171*, 191.
(15) Barton, D. G.; Soled, S. L.; Meitzner, G. D.; Fuentes, G. A.; Iglesia, E. *J. Catal*. **1999**, *181*, 57.
(16) Iglesia, E.; Barton, D. G.; Soled, S. L.; Miseo, S.; Baumgartner, J. E.; Gates, W. E.; Fuentes, G. A.; Meitzner, G. D. *Stud. Surf. Sci. Catal*. **1996**, *101*, 533.
(17) Larsen, G.; Lotero, E.; Raghavan, S.; Parra, R. D.; Querini, C. A. *Appl. Catal., A* **1996**, *139*, 201.
(18) Vaudagna, S. R.; Canavese, S. A.; Comelli, R. A.; Figoli, N. S. *Appl. Catal., A* **1998**, *168*, 93.
(19) Barton, D. G.; Shtein, M.; Wilson, R. D.; Soled, S. L.; Iglesia, E. *J. Phys. Chem. B* **1999**, *103*, 630.
(20) (a) Vaidyanathan, N. Ph.D. Thesis, University of Pittsburgh, 1998. (b) Vaidyanathan, N.; Hercules, D. M.; Houalla, M. *Anal. Bioanal. Chem*. **2002**, *373*, 547.
(21) Onfroy, T.; Clet, G.; Houalla, M. *Chem. Commun*. **2001**, 1378.
(22) Lahousse, C.; Aboulayt, A.; Maugé, F.; Bachelier, J.; Lavalley, J. C. *J. Mol. Catal*. **1993**, *84*, 283.
(23) Gazzoli, D.; Valigi, M.; Dragone, R.; Marucci, A.; Mattei, G. *J. Phys. Chem. B* **1997**, *101*, 11129.

(24) Scheithauer, M.; Grasselli, R. K.; Knözinger, H. *Langmuir* **1998**, *14*, 3019.
(25) Kim, B. K.; Hahn, J. W.; Han, K. R *J. Mater. Sci. Lett.* **1997**, *16*, 669.
(26) Onfroy, T.; Clet, G.; Houalla, M. Unpublished results.
(27) Valigi, M.; Gazzoli, D.; Cimino, A.; Proverbio, E. *J. Phys. Chem. B* **1999**, *103*, 11318.
(28) Vaidyanathan, N.; Hercules, D. M.; Houalla, M. *Surf. Interface Anal.* **1998**, *26*, 415.
(29) Zhao, B.; Xu, X.; Gao, J.; Fu, Q.; Tang, Y. *J. Raman Spectrosc.* **1996**, *27*, 549.
(30) Gutiérrez-Alejandre, A.; Castillo, P.; Ramirez, J.; Ramis, G.; Busca, G. *Appl. Catal., A* **2001**, *216*, 181.
(31) Wachs, I. E. *Catal. Today* **1996**, *27*, 437.
(32) Weckhuysen, B. M.; Jehng, J. M.; Wachs, I. E. *J. Phys. Chem. B* **2000**, *104*, 7382.
(33) Jacobs, P. A.; Heylen, C. F. *J. Catal.* **1974**, *34*, 267.
(34) Travert, A.; Manoilova, O. V.; Tsyganenko, A. A.; Maugé, F.; Lavalley, J. C. *J. Phys. Chem. B* **2002**, *106*, 1350.
(35) Hadjiivanov, K.; Vayssilov, G. N. *Adv. Catal.* **2002**, *47*, 307.
(36) Knözinger, H. In *Handbook of Heterogeneous Catalysis*; Ertl, G., Knözinger, H., Weitkamp, J., Eds.; Wiley-VCH: Weinheim, Germany, 1997; Vol. 2, p 707.
(37) Cairon, O.; Chevreau, T.; Lavalley, J. C. *J. Chem. Soc., Faraday Trans.* **1998**, *94*, 3039.
(38) Ferraris, G.; De Rossi, S.; Gazzoli, D.; Pettiti, I.; Valigi, M.; Magnacca, G.; Morterra, C. *Appl. Catal., A* **2003**, *240*, 119.
(39) Bolis, V.; Morterra, C.; Fubini, B.; Ugliengo, P.; Garrone, E. *Langmuir* **1993**, *9*, 1521.
(40) Fournier, M.; Louis, C.; Che, M.; Chaquin, P.; Masure, D. *J. Catal.* **1989**, *119*, 400.
(41) Weber, R. S. *J. Catal.* **1995**, *151*, 470.
(42) Valigi, M.; Gazzoli, D.; Pettiti, I.; Mattei, G.; Colonna, S.; De Rossi, S.; Ferraris, G. *Appl. Catal., A* **2002**, *231*, 159.
(43) Aramendia, M. A.; Borau, V.; Garcia, I. M.; Jiménez, C.; Marinas, A.; Marinas, J. M.; Porras, A.; Urbano, F. J. *Appl. Catal., A* **1999**, *184*, 115.
(44) Gervasini, A.; Auroux, A. *J. Catal.* **1991**, *131*, 190.
(45) Ouqour, A.; Coudurier, G.; Védrine, J. C. *J. Chem. Soc., Faraday Trans.* **1993**, *89*, 3151.
(46) Diez, V. K.; Apesteguia, C. R.; Di Cosimo, J. I. *J. Catal.* **2003**, *215*, 220.
(47) Kulkarni, D.; Wachs, I. E. *Appl. Catal., A* **2002**, *237*, 121.
(48) Knözinger, H.; Buhl, H.; Ress, E. *J. Catal.* **1968**, *12*, 121.
(49) Haffad, D.; Chambellan, A.; Lavalley, J. C. *J. Mol. Catal. A* **2001**, *168*, 153.
(50) Knözinger, H. *Angew. Chem., Int. Ed. Engl.* **1968**, *7*, 791.
(51) Wang, L.; Hall, W. K. *J. Catal.* **1982**, *77*, 232.
(52) Lambert, J.-F.; Che, M. *J. Mol. Catal. A* **2000**, *162*, 5.
(53) Karakonstantis, L.; Bourikas, K.; Lycourghiotis, A. *J. Catal.* **1996**, *162*, 295.
(54) Eibl, S.; Gates, B. C.; Knözinger, H *Langmuir* **2001**, *117*, 107.
(55) Prinetto, F.; Cerrato, G.; Ghiotti, G.; Chiorino, A.; Campa, M. C.; Gazzoli, D.; Indovina, V. *J. Phys. Chem. B* **1995**, *99*, 5556.
(56) Toda, Y.; Ohno, T.; Hatayama, F.; Miyata, H. *Appl. Catal., A* **2001**, *207*, 273.
(57) Ostromecki, M. M.; Burcham, L. J.; Wachs, I. E.; Ramani, N.; Ekerdt, J. G. *J. Mol. Catal. A* **1998**, *132*, 43.
(58) Naito, N.; Katada, N.; Niwa, M. *J. Phys. Chem. B* **1999**, *103*, 7206.
(59) Shimizu, K.; Venkatraman, T. N.; Song, W. *Appl. Catal., A* **2002**, *224*, 77.
(60) Baertsch, C. D.; Soled, S. L.; Iglesia, E. *J. Phys. Chem. B* **2001**, *105*, 1320.
(61) Onfroy, T.; Clet, G.; Bukallah, S. B.; Hercules, D. M.; Houalla, M. *Catal. Lett.* **2003**, *89*, 15.
(62) De Rossi, S.; Ferraris, G.; Valigi, M.; Gazzoli, D. *Appl. Catal., A* **2002**, *231*, 173.
(63) Turek, A. M.; Wachs, I. E.; DeCanio, E. *J. Phys. Chem.* **1992**, *96*, 5000.
(64) Onfroy, T.; Clet, G.; Bukallah, S. B.; Houalla, M. *13th ICC, Paris (France)* **2004**, *Poster P1−446*.
(65) Villanneau, R.; Carabineiro, H.; Carrier, X.; Thouvenot, R.; Herson, P.; Lemos, F.; Ramôa Ribeiro F.; Che, M. *J. Phys. Chem. B* **2004**, *108*, 12465.